

# From Groups to Particle Colliders: The Search for Fractionally Charged Particles

Florian Muennich

Supervisor: Dr. Rodrigo Alonso

Department of Physics, Durham University



July 2025

# 1 Introduction

In 1909, Millikan and Fletcher made the first precision measurement of the charge of an electron, for which Millikan won the Nobel Prize [1]. In the 116 years since, the so-called 'elementary charge' or  $e$  has remained just that - elementary. As far as we know, no smaller quantum of charge exists. Why is this the case, and must it be so? Quantisation is one of the most important ideas of 20th century physics, but is a rather simple concept: our universe is made up of elementary building blocks, or 'quanta'. The most familiar case of quantisation is that of matter: you can't keep cutting matter into smaller and smaller pieces, for eventually you will be left with elementary particles, such as electrons, quarks, and so on. Quantisation applies to energy, as revealed by Planck's  $E = h\nu$  and supported by Einstein's discovery of the photoelectric effect, for which he won the Nobel Prize in 1921.

So what about charge? It appears logical to conclude that it is also quantised in units of the electron charge  $e$ , given that all charged particles measured in experiment have had charges  $ne$ , where  $n$  is an integer. Nevertheless, modern physics does not explicitly require charge quantisation, and 'fractionally charged particles' (FCPs) could well exist. Critically, their discovery could help us understand more about the standard model's group structure. Determining the Standard Model's true group structure would encode all we know about the interactions of particles with the key fundamental forces (excluding gravity).

This research project analyses the ongoing search for fractionally charged particles (FCPs), connecting abstract maths which describes the Standard Model to concrete experimental results. These could, in principle, have a charge that is any non-integer multiple of  $e$ , but as the vast majority of experiments examine only  $|Q| < e$ , only that region will be examined.

## 2 Theory

### 2.1 A note on Group Theory

Group theory underpins much of modern physics, and is critical to this project. The Standard Model's group structure encodes nearly all the information we have about the mechanisms of electromagnetism, the weak force, and the strong force. It also determines what the smallest possible charge could be - the issue is, there are a number of equally possible candidates for the SM group [4]. Due to the complexity of how charge arises from the SM group, I will use the example of two straightforward groups,  $SO(3)$  and  $SU(2)$ , to illustrate the connection between FCPs and the group structure of the Standard Model.

This theory section will assume a basic understanding of group theory - what a group is, group isomorphisms, Lie algebras. For those interested or unfamiliar with this area, see [2] for a quick introduction or [3] for an in-depth breakdown.

## 2.2 SO(3) and SU(2)

Two fairly straightforward groups with important applications in physics are SO(3) and SU(2). SO(3) consists of  $3 \times 3$  special orthogonal matrices, which satisfy  $R^T R = \mathbb{I}, \det(R) = 1$ . This can be visualised as the set of rotations in 3-dimensional [real] space. If you pick up any object, and rotate it about its centre in some way, that rotation is an element of SO(3). SU(2) consists of  $2 \times 2$  special unitary matrices, which satisfy  $U^\dagger U = \mathbb{I}, \det(U) = 1$ . This is the set of rotations in 2-dimensional complex space. It seems far more abstract than SO(3), but they are closely related.

SU(2) and SO(3) are Lie groups, thus any element of either group can be written as an exponential. For  $U \in SU(2), U = e^{i\alpha T}$ , where  $\alpha$  is some phase and  $T$  is another matrix. Similarly, we can write  $R \in SO(3)$  as  $e^{i\beta T}$ , where the parameter is  $\beta$  rather than  $\alpha$ . So, each  $U$  or  $R$  has a corresponding  $T$ , which we call a *generator* of the group.

These generators form a vector space, and therefore it is useful to write a corresponding basis. This can be derived by applying the group properties and Taylor-expanding the exponentiated form (see appendix). For SU(2), this basis is the set of Pauli matrices

$$\left\{ \begin{bmatrix} 0 & 1 \\ 1 & 0 \end{bmatrix}, \begin{bmatrix} 0 & -i \\ i & 0 \end{bmatrix}, \begin{bmatrix} 1 & 0 \\ 0 & -1 \end{bmatrix} \right\},$$

which are denoted  $\sigma_i, i \in \{1, 2, 3\}$ .

For SO(3), the basis is formed by

$$\left\{ \begin{bmatrix} 0 & -i & 0 \\ i & 0 & 0 \\ 0 & 0 & 0 \end{bmatrix}, \begin{bmatrix} 0 & 0 & i \\ 0 & 0 & 0 \\ -i & 0 & 0 \end{bmatrix}, \begin{bmatrix} 0 & 0 & 0 \\ 0 & 0 & -i \\ 0 & i & 0 \end{bmatrix} \right\}.$$

The generators of the groups do not appear obviously related. Another level of abstraction must be introduced, namely the Lie algebra, defined by the commutator bracket. For SU(2),

$$[\sigma_1, \sigma_2] = \sigma_1 \sigma_2 - \sigma_2 \sigma_1 = \begin{bmatrix} 0 & 1 \\ 1 & 0 \end{bmatrix} \begin{bmatrix} 0 & -i \\ i & 0 \end{bmatrix} - \begin{bmatrix} 0 & -i \\ i & 0 \end{bmatrix} \begin{bmatrix} 0 & 1 \\ 1 & 0 \end{bmatrix} = 2 \begin{bmatrix} i & 0 \\ 0 & -i \end{bmatrix} = 2i\sigma_3.$$

This pattern is repeated, so in general we can say that  $[\sigma_i, \sigma_j] = 2i \sum_{k=1}^3 \epsilon_{ijk} \sigma_k$ .

SO(3) has the following commutator relation:

$$[T_1, T_2] = \begin{bmatrix} 0 & -i & 0 \\ i & 0 & 0 \\ 0 & 0 & 0 \end{bmatrix} \begin{bmatrix} 0 & 0 & i \\ 0 & 0 & 0 \\ -i & 0 & 0 \end{bmatrix} - \begin{bmatrix} 0 & 0 & i \\ 0 & 0 & 0 \\ -i & 0 & 0 \end{bmatrix} \begin{bmatrix} 0 & -i & 0 \\ i & 0 & 0 \\ 0 & 0 & 0 \end{bmatrix} = \begin{bmatrix} 0 & 0 & 0 \\ 0 & 0 & 1 \\ 0 & -1 & 0 \end{bmatrix} = iT_3,$$

and thus  $[T_i, T_j] = i \sum_{k=1}^3 \epsilon_{ijk} T_k$ . Now, the parallels between the two groups should be clear: their commutator relations differ only by a factor of 2.

This numerical factor clearly arises from our choice of the arbitrary 'phases'  $\beta$  and  $\alpha$ , so the Lie algebra of SU(2) and SO(3) is essentially the same. In order to better compare the groups, we can normalise our Lie algebras by setting

$$\mathfrak{so}(3) = \mathfrak{su}(2) = i \sum_{k=1}^3 \epsilon_{ijk} T_k.$$

In practice, this requires rescaling the SU(2) generators by a factor of 1/2. We may then write

$$U = e^{i\alpha\sigma} = e^{i\frac{\beta}{2}\sigma},$$

so that both SO(3) and SU(2) are parametrised by  $\beta$ , and are thus directly comparable.

## 2.3 General forms of the Fundamental Representation

The generators can then be used to obtain the fundamental representations of SU(2) and SO(3) by actually Taylor expanding the exponentials. This could be done separately for each basis generator, which would produce a basis set of matrices for the fundamental representation. One would obtain

$$\begin{bmatrix} \cos \alpha & \sin \alpha \\ -\sin \alpha & \cos \alpha \end{bmatrix}$$

for SU(2) and

$$\left\{ \begin{bmatrix} \cos \beta & \sin \beta & 0 \\ -\sin \beta & \cos \beta & 0 \\ 0 & 0 & 1 \end{bmatrix}, \begin{bmatrix} \cos \beta & 0 & \sin \beta \\ 0 & 1 & 0 \\ -\sin \beta & 0 & \cos \beta \end{bmatrix}, \begin{bmatrix} 1 & 0 & 0 \\ 0 & \cos \beta & \sin \beta \\ 0 & -\sin \beta & \cos \beta \end{bmatrix} \right\}$$

for SO(3). These matrices should look familiar - they are the  $2 \times 2$  and  $3 \times 3$  rotation matrices, describing rotations around the  $x$  and  $y, z$  axes respectively, by angles  $\alpha$  and  $\beta$ .

A more useful formulation, however, would be one that describes *any* 3-dimensional rotation. Thus, we must exponentiate the generators not individually, but as a linear combination. This also means we need 3 parameters, as we can rotate by any angle independently around 3 axes.

For SU(2) we can rewrite  $U = e^{i\alpha_i\sigma_i}$ , where we sum over  $i = \{1, 2, 3\}$ . Thus:

$$U = e^{i\alpha_i\sigma_i} = \exp\left(i\alpha_1 \begin{bmatrix} 0 & 1 \\ 1 & 0 \end{bmatrix} + i\alpha_2 \begin{bmatrix} 0 & -i \\ i & 0 \end{bmatrix} + i\alpha_3 \begin{bmatrix} 1 & 0 \\ 0 & -1 \end{bmatrix}\right) = \exp\left(i \begin{bmatrix} \alpha_3 & \alpha_1 - i\alpha_2 \\ \alpha_1 + i\alpha_2 & -\alpha_3 \end{bmatrix}\right)$$

This we can Taylor expand, as in the previous section. The result of this is

$$U = \left(\sum_{n=0}^{\infty} \frac{(-1)^n}{2n!} (\alpha_1^2 + \alpha_2^2 + \alpha_3^2)^n\right) \cdot \mathbb{I} + i \left(\sum_{n=0}^{\infty} \frac{(-1)^n}{(2n+1)!} (\alpha_1^2 + \alpha_2^2 + \alpha_3^2)^n\right) \begin{bmatrix} \alpha_3 & \alpha_1 - i\alpha_2 \\ \alpha_1 + i\alpha_2 & -\alpha_3 \end{bmatrix}$$

$$= \cos\left(\sqrt{\alpha_1^2 + \alpha_2^2 + \alpha_3^2}\right) \cdot \mathbb{I} + \frac{i \sin\left(\sqrt{\alpha_1^2 + \alpha_2^2 + \alpha_3^2}\right)}{\sqrt{\alpha_1^2 + \alpha_2^2 + \alpha_3^2}} \begin{bmatrix} \alpha_3 & \alpha_1 - i\alpha_2 \\ \alpha_1 + i\alpha_2 & -\alpha_3 \end{bmatrix}$$

By replacing  $\sqrt{\alpha_1^2 + \alpha_2^2 + \alpha_3^2}$  with  $|\alpha|$ , we can finally write

$$U = \begin{bmatrix} \cos|\alpha| + i\frac{\alpha_3}{|\alpha|} \sin|\alpha| & \frac{\alpha_2 + i\alpha_1}{|\alpha|} \sin|\alpha| \\ -\frac{\alpha_2 + i\alpha_1}{|\alpha|} \sin|\alpha| & \cos|\alpha| - i\frac{\alpha_3}{|\alpha|} \sin|\alpha| \end{bmatrix}$$

and we can check that this does indeed hold for our previous, special cases when only one  $\alpha_i$  is non-zero.

Similarly, we can obtain a general matrix representation of  $\text{SO}(3)$ , which is slightly more arduous due to its generators being  $3 \times 3$  matrices. We can write

$$\begin{aligned} O = e^{i\beta_i u_i} &= \exp\left(\beta_1 \begin{bmatrix} 0 & 0 & 0 \\ 0 & 0 & -1 \\ 0 & 1 & 0 \end{bmatrix} + \beta_2 \begin{bmatrix} 0 & 0 & 1 \\ 0 & 0 & 0 \\ -1 & 0 & 0 \end{bmatrix} + \beta_3 \begin{bmatrix} 0 & -1 & 0 \\ 1 & 0 & 0 \\ 0 & 0 & 0 \end{bmatrix}\right) \\ &= \exp \begin{bmatrix} 0 & -\beta_3 & \beta_2 \\ \beta_3 & 0 & -\beta_1 \\ -\beta_2 & \beta_1 & 0 \end{bmatrix} \end{aligned}$$

Once again Taylor expanding, we get

$$\begin{aligned} O &= \mathbb{I} + \frac{1 - \cos|\beta|}{|\beta|^2} \begin{bmatrix} -\beta_2^2 - \beta_3^2 & \beta_1\beta_2 & \beta_1\beta_3 \\ \beta_1\beta_2 & -\beta_1^2 - \beta_3^2 & \beta_2\beta_3 \\ \beta_1\beta_3 & \beta_2\beta_3 & -\beta_1^2 - \beta_2^2 \end{bmatrix} + \frac{\sin|\beta|}{|\beta|} \begin{bmatrix} 0 & -\beta_3 & \beta_2 \\ \beta_3 & 0 & -\beta_1 \\ -\beta_2 & \beta_1 & 0 \end{bmatrix} \\ &= \begin{bmatrix} 1 + \frac{|\beta|^2 - \beta_1^2}{|\beta|^2} (\cos|\beta| - 1) & \frac{\beta_1\beta_2}{|\beta|^2} (1 - \cos|\beta|) - \frac{\beta_3}{|\beta|} \sin|\beta| & \frac{\beta_1\beta_3}{|\beta|^2} (1 - \cos|\beta|) + \frac{\beta_2}{|\beta|} \sin|\beta| \\ \frac{\beta_1\beta_2}{|\beta|^2} (1 - \cos|\beta|) + \frac{\beta_3}{|\beta|} \sin|\beta| & 1 + \frac{|\beta|^2 - \beta_2^2}{|\beta|^2} (\cos|\beta| - 1) & \frac{\beta_2\beta_3}{|\beta|^2} (1 - \cos|\beta|) - \frac{\beta_1}{|\beta|} \sin|\beta| \\ \frac{\beta_1\beta_3}{|\beta|^2} (1 - \cos|\beta|) - \frac{\beta_2}{|\beta|} \sin|\beta| & \frac{\beta_2\beta_3}{|\beta|^2} (1 - \cos|\beta|) + \frac{\beta_1}{|\beta|} \sin|\beta| & 1 + \frac{|\beta|^2 - \beta_3^2}{|\beta|^2} (\cos|\beta| - 1) \end{bmatrix} \end{aligned}$$

returning a general form of the fundamental representation of  $\text{SO}(3)$ , which also returns the basis matrices when we choose only one  $\beta_i$  to be non-zero.

## 2.4 Proof of $\text{SU}(2)$ - $\text{SO}(3)$ double cover

In this section, I will demonstrate an intuitive approach to proving the global relationship between  $\text{SU}(2)$  and  $\text{SO}(3)$ , which I devised during my project.

In order to compare the general matrix forms of SU(2) and SO(3), the equivalence relation  $\alpha = \frac{\beta}{2}$  must be applied. Thus the general SU(2) matrix can be written as:

$$U = \begin{bmatrix} \cos \frac{|\beta|}{2} + i \frac{\beta_3}{|\beta|} \sin \frac{|\beta|}{2} & \frac{\beta_2 + i\beta_1}{|\beta|} \sin \frac{|\beta|}{2} \\ -\frac{\beta_2 + i\beta_1}{|\beta|} \sin \frac{|\beta|}{2} & \cos \frac{|\beta|}{2} - i \frac{\beta_3}{|\beta|} \sin \frac{|\beta|}{2} \end{bmatrix}$$

If there exists a transformation  $\beta_i \rightarrow \beta'_i$  such that the SO(3) matrix is invariant, while SU(2) is not, this would demonstrate that any SO(3) element maps to multiple SU(2) elements, and hence SU(2) is a universal covering group of SO(3). If this transformation can be applied again and the SU(2) matrix reverts to its original form, then the correspondence is clearly 2-1. Given the use of a general matrix, this is a proof of the fact that SU(2) is the double cover of SO(3).

A transformation that leaves all sines and cosines invariant in the SO(3) matrix is  $|\beta| \rightarrow |\beta| + 2\pi$ . The coefficients must also all remain invariant, thus the condition

$$\frac{|\beta|^2 - \beta_1^2}{|\beta|^2} = \frac{|\beta'|^2 - \beta_1'^2}{|\beta'|^2} = \frac{(|\beta| + 2\pi)^2 - \beta_1'^2}{(|\beta| + 2\pi)^2}$$

$$1 - \frac{\beta_1^2}{|\beta|^2} = 1 - \frac{\beta_1'^2}{(|\beta| + 2\pi)^2} \rightarrow \beta_1'^2 = \frac{\beta_1^2}{|\beta|^2} (|\beta| + 2\pi)^2$$

can be imposed. This is not unique to  $\beta_1$ , but applies generally to  $\beta_i$ . We can check this is indeed consistent with the original transformation  $|\beta| \rightarrow |\beta| + 2\pi$ :

$$|\beta'| = \sqrt{\frac{\beta_1^2}{|\beta|^2} (|\beta| + 2\pi)^2 + \frac{\beta_2^2}{|\beta|^2} (|\beta| + 2\pi)^2 + \frac{\beta_3^2}{|\beta|^2} (|\beta| + 2\pi)^2} = \frac{(|\beta| + 2\pi)}{|\beta|} \sqrt{\beta_1^2 + \beta_2^2 + \beta_3^2} = |\beta| + 2\pi.$$

The transformation  $\beta_i \rightarrow \beta_i(1 + \frac{2\pi}{|\beta|})$  clearly leaves SO(3) invariant. Applying the same transformation to SU(2), one obtains

$$U' = \begin{bmatrix} \cos \frac{|\beta|+2\pi}{2} + i \frac{\beta_3}{|\beta|} \sin \frac{|\beta|+2\pi}{2} & \frac{\beta_2 + i\beta_1}{|\beta|} \sin \frac{|\beta|+2\pi}{2} \\ -\frac{\beta_2 + i\beta_1}{|\beta|} \sin \frac{|\beta|+2\pi}{2} & \cos \frac{|\beta|+2\pi}{2} - i \frac{\beta_3}{|\beta|} \sin \frac{|\beta|+2\pi}{2} \end{bmatrix}.$$

The argument increases by  $\pi$ , and hence a minus sign is introduced in front of each sine and cosine:  $U' = -U$ . Applying the transformation again:  $(-U) \rightarrow -(-U) = U$ . Hence, for every element  $R$ , there are two elements  $U$  and  $-U$ . This is proof that SU(2) is the double-cover of SO(3).

The transformation  $\beta_i \rightarrow \beta_i(1 + \frac{2\pi}{|\beta|})$  does appear to be problematic in the limit  $|\beta| \rightarrow 0$ , seemingly introducing a singularity. However, this is not actually problematic. The matrices  $U$  and  $R$  are defined in terms of elements which have well-behaved limits as  $|\beta| \rightarrow 0$  (using the standard Taylor expansions). In this limit,  $U, R \rightarrow \mathbb{I}$ , so both smoothly reduce to the identity matrix. Then under the transformation, we simply have  $U = \mathbb{I} \rightarrow -\mathbb{I}$  and  $R$  naturally remains invariant.

Seen differently, removing the distinction between  $U$  and  $-U$  gives SO(3). This can be formalised using the group  $\mathbb{Z}_2 = [-1, 1]$ , which allows SO(3) to be expressed as a quotient group of SU(2):

$$SO(3) = \frac{SU(2)}{\mathbb{Z}_2}.$$

Thus,  $SU(2)$  and  $SO(3)$  are very similar on an abstract level, with the distinction that  $SU(2)$  is the double-cover of  $SO(3)$ .

## 2.5 From Abstract Groups to Quantisation

How is this relevant to charge quantisation and the Standard Model? Physical quantities like charge and colour have related fields with underlying group structures. The group properties, then, have an effect on how these quantities are generated.

In the Standard Model, electric charge is the sum of two quantum numbers, and is thus generated by two groups.  $SU(2)$  provides the weak isospin generator  $T_3$ , and  $U(1)$  generates the weak hypercharge  $Y$ . Charge is then defined by the Gell-Mann-Nishijima relation:

$$Q = T_3 + \frac{Y}{2} \quad (1)$$

This adds a level of complexity to charge generation that is not appropriate for this research. Instead, this section uses the example of spin, which is generated by  $SU(2)$ , to illustrate how global group structure affects quantisation of spin, and by analogy, charge.

Quantum numbers are generated from Lie groups by their Cartan subalgebra. This arises because quantum numbers are conserved, and hence must be generated by an Abelian algebra, which is the Cartan subalgebra in the case of Lie groups. Equivalently, it is the subset of diagonalisable generators. The quantum numbers generated by a Lie group are the eigenvalues of this subalgebra.

Consider a particle with state  $|\psi\rangle$ , acted on by a spin operator of the form  $e^{i\alpha T}$ . It will transform as

$$|\psi\rangle \rightarrow e^{i\alpha T} |\psi\rangle \simeq (\mathbb{I} + i\alpha T + \dots) |\psi\rangle$$

where  $T$  is an element of the Cartan subalgebra.

All fermions (electrons, neutrinos, quarks, etc.), have a corresponding state  $|\psi\rangle = \begin{pmatrix} \psi_\uparrow \\ \psi_\downarrow \end{pmatrix}$ . Naturally,  $T$  must then be a  $2 \times 2$  Cartan generator - meaning spin is generated simply by  $SU(2)$  in this case. The Cartan subalgebra consists of just  $\sigma_3$ , so

$$|\psi\rangle \rightarrow e^{i\frac{\beta}{2}\sigma_3} |\psi\rangle \approx \left( \mathbb{I} + i\beta \begin{bmatrix} \frac{1}{2} & 0 \\ 0 & -\frac{1}{2} \end{bmatrix} + \dots \right) |\psi\rangle.$$

The eigenvalues of the Cartan generator, and thus base units of spin, are  $\pm\frac{1}{2}$ .

On the other hand, vector bosons (W, Z, gluons) have corresponding states  $|\psi\rangle = \begin{pmatrix} \psi_1 \\ \psi_0 \\ \psi_{-1} \end{pmatrix}$  which

must transform under the  $3 \times 3$  representation of  $SU(2)$ . This *is*  $SO(3)$ . Choosing  $T_3$  as the Cartan generator, it diagonalises to

$$T_3 = \begin{bmatrix} 1 & 0 & 0 \\ 0 & 0 & 0 \\ 0 & 0 & -1 \end{bmatrix}.$$

The corresponding transformation is

$$|\psi\rangle \longrightarrow e^{i\beta T_3} |\psi\rangle \approx \left( \mathbb{I} + i\beta \begin{bmatrix} 1 & 0 & 0 \\ 0 & 0 & 0 \\ 0 & 0 & -1 \end{bmatrix} + \dots \right) |\psi\rangle,$$

yielding eigenvalues  $\pm 1, 0$  as the fundamental spin unit.

The fact that  $SU(2)$  is the double cover of  $SO(3)$  thus leads to a difference in quantisation. The key point is that *global* group properties can affect the quantisation of conserved quantum numbers.

Critically,  $SU(2)$  is the true *true* spin group.  $SO(3)$  generates spin for vector bosons, but only because it is the 3-dimensional representation of  $SU(2)$ . Were one to observe solely vector bosons, one would only observe integer spin. This would lead to an ambiguity in terms of the underlying spin group: it could be  $SO(3)$ , or  $SU(2)$  [restricted to these groups because we know what the Lie algebra is]. The observation of fermions, with spin- $\frac{1}{2}$ , resolves this ambiguity, as  $SO(3)$  cannot generate a half-integer spin.  $SU(2)$  is the underlying group.

## 2.6 FCPs and the SM Gauge Group

This ambiguity is what plagues the standard model group: currently, it is as if fermions had not been discovered. The Lie algebra of the Standard Model group is known, but which of the corresponding locally-isomorphic groups is the underlying, true SM group is not, as only integer charges have been observed so far. The SM gauge group can be written as:

$$G_p = \frac{SU(3)_C \times SU(2)_L \times U(1)_Y}{\mathbb{Z}_p}, p \in \{1, 2, 3, 6\} \quad (2)$$

where  $SU(3)$  describes strong interactions,  $SU(2)$  weak interactions, and  $U(1)$  electromagnetic interactions. These 4 groups are locally isomorphic, so the observation of integer charges cannot tell them apart, but the observation of smaller charge quanta could. The unit charges permitted by each candidate are shown below.

$p$	Charge Quantum
1	$\frac{1}{6}$
2	$\frac{1}{3}$
3	$\frac{1}{2}$
6	1

This is just a slightly more complex version of  $SO(3)$  and  $SU(2)$ : Just as  $SU(2)$  is the double cover of  $SO(3)$ ,  $G_3$  is the double cover of  $G_6$ ,  $G_2$  is its triple cover, and  $G_1$  is its sextuple cover.

Just as the observation of a particle with  $\frac{1}{2}$  integer spin would discount  $SO(3)$  as the underlying group in the example above, the discovery of any FCP would immediately remove  $G_6$  as a possibility. However, this would not necessarily single out the true SM group. A particle of charge  $\frac{1}{2}e$  or  $\frac{1}{3}e$  would still be consistent with a unit charge of  $\frac{1}{6}e$ . Thus it is only if the true SM group is  $G_1$  **and** a particle with charge  $\frac{1}{6}e$  or  $\frac{5}{6}e$  is observed that FCP observation would single out the true SM group. Nevertheless, the potential for narrowing down the candidate pool is attractive.

Beyond potentially revealing the underlying charge quantisation in nature, the discovery of an FCP could be useful in Beyond the Standard Model (BSM) physics. A number of GUTs have been proposed, but finding the right one is even harder than finding the right SM gauge group.  $G_p$  must be a subgroup of any GUT gauge group, and thus the restriction of  $p$  could restrict the possible GUTs. This would be highly significant. For example, two of the most prominent GUT candidates,  $SU(5)$  and  $SO(10)$ , are only compatible with  $G_6$ . The observation of any FCP would discount these.

### 3 Experiment Types

The search for fractionally charged particles has employed a number of different experimental methods over the years. Broadly, we can split searches into direct detection (DD) and cosmological searches. The results of direct detection experiments are more reliable than the latter and will be examined first.

#### 3.1 Direct Detection

Direct Detection experiments look to actually observe an FCP. Perhaps the most familiar DD experiments would be particle colliders, such as the LHC. Particle colliders are particularly useful for constraining high mass, non-millicharged FCPs. High energies can be attained in colliders such as the LHC, while the trade-off for this is poor sensitivity to lower charges (currently  $\sim q < \frac{1}{3}e$ ).

Another effective method of searching is external detection at colliders. These are small detectors placed at a distance from the collider interaction point, usually separated by concrete. These exper-

iments have the advantage of being able to detect very small charges (i.e. millicharged particles). However, they can only detect slow-moving particles, which means high energies cannot realistically be reached. This demonstrates the major limitation of DD experiments: the inverse relationship between energy and sensitivity. This makes it very hard to probe low charges for high masses, and vice-versa.

There are further types of DD experiments, such as neutrino detectors, but these merit their own study, which falls beyond the bounds of this paper.

### 3.2 Cosmology-based Bounds

The most stringent bounds so far have been obtained by use of cosmological arguments. It is theorised that FCPs could have been produced in the reheating era  $\sim 10^{-34}$  s after the Big Bang[5]. These FCPs could also have extremely small charges (denoted mCPs), but these are less relevant to the project as they would not have a direct link to the SM gauge group.

While the constraints obtained by cosmological arguments are superior to DD bounds, they should also be approached with some caution. They do not directly detect FCPs, so the limits rely on the quality of the inferences made from the CMB. Critically, these bounds assume that the FCPs were produced in the early universe - and thus assuming the universe was hot enough at the right time to produce a given FCP. Given that neither the maximum temperature reached in reheating nor the exact time at which it happened is known, this assumption should not be taken for granted. Moreover, given that DD experiments can exclude most lower energies, cosmological constraints are most interesting regarding higher energies. The assumption that FCPs were produced at these higher energies is even more tenuous than at lower ones, thus the relevant cosmological bounds are less reliable.

## 4 Methodology

Exclusion limits were obtained from existing analyses of experimental searches for fractionally charged particles (FCPs), rather than from raw data. Due to the timescale, broad scope of this study and the significant variation among experimental methodologies — ranging from collider-based to cosmological approaches — independent data analysis was neither feasible nor necessary. Exclusion bounds were extracted from published figures using PlotDigitizer, an online tool for digitising graphical data. Calibration points were selected to be as widely separated as possible, improving the accuracy of the data collection. The extracted data points were subsequently imported into Python and visualised using the matplotlib.pyplot library.

Although data from both collider/reactor and cosmological experiments were collected, only the former were used in the construction of final exclusion limits. While all FCP searches involve assumptions (e.g. collider experiments assume Drell-Yan production), those involved in obtaining cosmological bounds were deemed too speculative to be taken at face value. Accordingly, regions excluded solely on the basis of cosmological models were included in the plots but shaded in a lighter grey.

An additional consideration was the assumed spin of the target particles in each experiment. In the absence of direct evidence, FCPs may be either fermions or bosons. This distinction can affect the resulting bounds by a non-negligible scale factor ( $> 10$ ) [4]. However, none of the experiments surveyed explicitly targeted bosonic FCPs; most assumed fermionic candidates or made no specification. As a result, no spin-based rescaling of exclusion limits was necessary.

The compiled exclusion plot was used to extract compounded bounds for specific fractional charges of interest:  $Q/e = \frac{1}{6}, \frac{1}{3}, \frac{1}{2}, \frac{2}{3}, \frac{5}{6}$ . For each of these values, the corresponding mass constraints were plotted individually to identify unconstrained or weakly constrained regions in parameter space. These gaps highlight areas where experimental sensitivity remains limited and thus served as the basis for formulating recommendations for future FCP searches.

## 5 Results

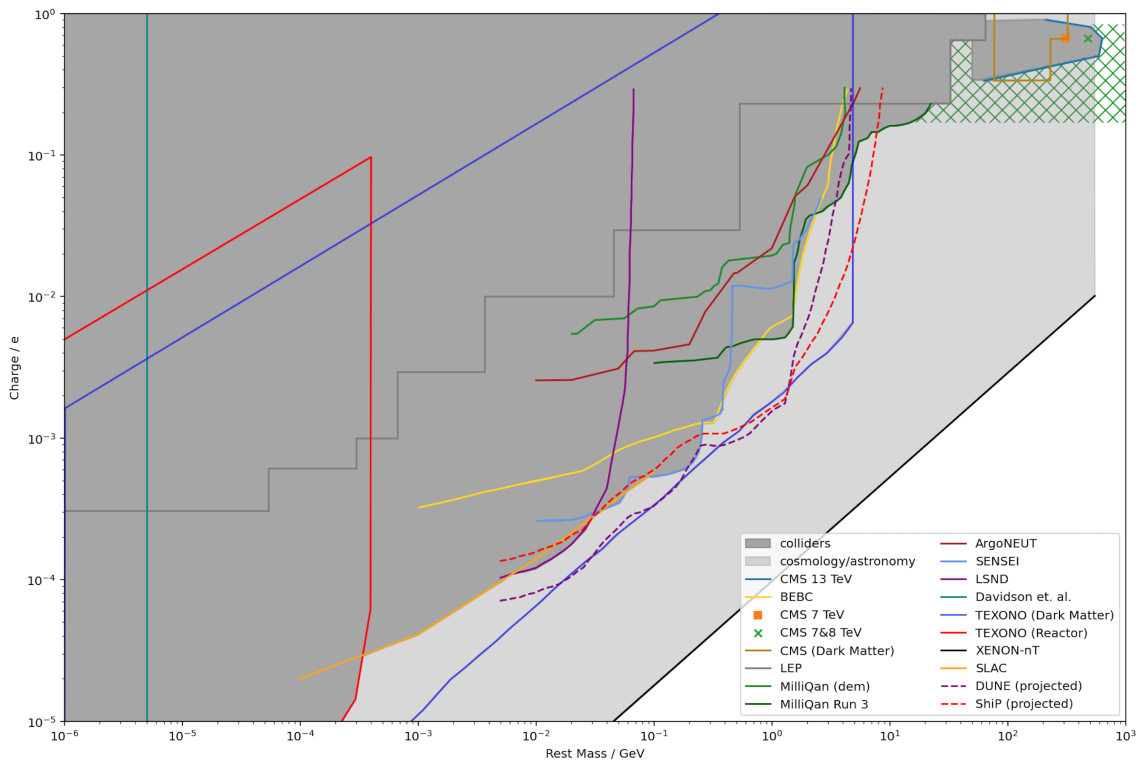


**Figure 1:** Exclusion limits of charge against mass for FCPs. The dark area is bounded by concrete experimental constraints ([6] - [16]), while the light grey area indicates limits based on cosmological models ([16] - [18]). The green hatched area indicates unprobed parameter space for particles consistent with an SM gauge group  $G_p$ . Projected bounds for ongoing/future experiments are dashed.

The combined exclusion limits are presented in Fig. 1, highlighting the experimental reach of searches for FCPs at different charges. There is a clear inverse relationship between charge sensitivity and mass, with mCP-focused experiments unable to probe masses over  $\sim 10$  GeV and colliders sensitive down to only  $\sim 0.3e$ .

Fortunately, the high-energy CMS searches cover the majority of charge values most relevant to this research. Only  $q = \frac{1}{6}e$  isn't covered, leading to weaker constraints on FCPs at this charge.

The combined bounds (DD only) were then extracted from Fig. 1, compiled in the table below and visualised in Fig. 2.

$Q/e$	Excluded $m$ / GeV
$\frac{1}{6}$	$< 14$
$\frac{1}{3}$	$< 33, 50 - 600$
$\frac{1}{2}$	$< 33, 50 - 595$
$\frac{2}{3}$	$< 640$
$\frac{5}{6}$	$< 405$

Excluded masses for fractional charges consistent with  $G_p$  candidates.

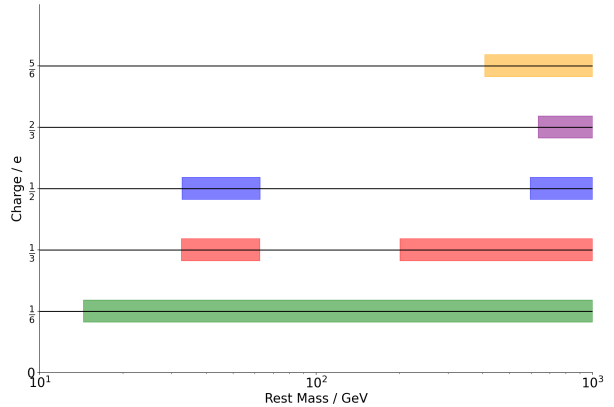


**Figure 2:** Exclusion limits for potential FCP charges relevant to SM group. Shaded regions represent parameter space not yet excluded by DD experiments.

Exclusion limits for  $q/e = \frac{1}{6}$  trail the others by a significant margin, due to the lack of sensitivity of CMS to lower charges: these bounds were obtained by MilliQan.  $q/e = \frac{1}{3}$  also trails the other upper limits noticeably, while there is a 'pocket' for  $q/e = \frac{1}{3}, \frac{1}{2}$  in the region 30 – 50 GeV which remains unprobed by DD experiments.

## Future Experimental Directions

I identify key directions for future experimental exploration in the search for FCPs.

### 1. Extending CMS-level energy searches to lower charges ( $q = \frac{1}{6}e$ )

Current mass exclusion limits for particles with charge  $q = \frac{1}{6}e$  significantly lag behind those for  $q \geq \frac{1}{3}e$ , with constraints typically only up to  $\sim 15$  GeV. This discrepancy arises because the best constraints on  $\frac{1}{6}e$  charges are set by the dedicated millicharged particle detector *MilliQan*, located

approximately 30 m from the CMS interaction point. While *MilliQan* is specifically optimized for detecting particles with very small ionization signals and low charges, it is only sensitive to slow-moving particles and cannot match the energy reach of CMS.

At CMS, FCPs are primarily identified via their small specific energy loss  $dE/dx$ , as their low electric charge causes them to be only weakly ionizing. However, CMS tracking detectors have a detection threshold set by the response to minimum ionizing particles (MIPs), below which signals are not reliably recorded. This places a lower bound on the detectable charge, currently around  $\frac{1}{3}e$ .

To probe charges below  $\frac{1}{3}e$ , two strategies are conceivable: increasing the sensitivity of CMS to lower ionization signals, or enabling *MilliQan* (or a similar detector) to access higher energies. The former is significantly more feasible in the near term and can be achieved through the increase in integrated luminosity at the LHC for Run 3 and the HL-LHC.

The expected number of FCP events,  $N_{\text{pred}}$ , expected to be less than 1 (as we have not detected any yet), is given by:

$$N_{\text{pred}} = \sigma_{\chi\bar{\chi}}\mathcal{L} = Q^2\sigma_0\mathcal{L} < 1, \quad (3)$$

where  $\sigma_{\chi\bar{\chi}}$  is the production cross section for FCPs, assumed to scale as  $Q^2$  relative to a known cross section  $\sigma_0$  (e.g., for muons), and  $\mathcal{L}$  is the integrated luminosity. From this, the minimum detectable charge scales as:

$$Q_{\text{min}} = \frac{1}{\sqrt{\sigma_0\mathcal{L}}} \Rightarrow Q_{\text{min}} \propto \frac{1}{\sqrt{\mathcal{L}}}. \quad (4)$$

During LHC Run 2 at 13 TeV, CMS collected an integrated luminosity of approximately  $160 \text{ fb}^{-1}$ , allowing sensitivity to charges down to  $Q_{\text{min}} \approx \frac{1}{3}e$ . Run 3 is expected to accumulate around  $300 \text{ fb}^{-1}$  by the end of 2026, suggesting potential sensitivity down to  $Q_{\text{min}} \approx \frac{1}{4}e$ . However, this still falls short of the desired  $\frac{1}{6}e$  target. The High Luminosity LHC (HL-LHC), projected to deliver  $3000 \text{ fb}^{-1}$ , would extend sensitivity to approximately  $Q_{\text{min}} \approx \frac{1}{13}e$ , comfortably covering the  $\frac{1}{6}e$  regime. Importantly, since the centre-of-mass energy will remain at 13–14 TeV, this improved sensitivity would permit exclusion (or discovery) of FCPs in this low-charge regime at higher masses than those currently accessible from *MilliQan*.

## 2. Exploring the parameter space $\frac{1}{3}e \leq q \leq \frac{2}{3}e$ , $30 \leq m_\chi \leq 50 \text{ GeV}$

This region represents an intriguing ‘‘pocket’’ in parameter space, bordered by existing exclusions at both lower and higher masses. Notably, it encompasses the values  $m_\chi \approx \frac{1}{2}m_Z \approx 45 \text{ GeV}$  and  $m_\chi \approx \frac{1}{4}m_H \approx 31 \text{ GeV}$ , where  $m_Z$  and  $m_H$  denote the masses of the Z boson and Higgs boson, respectively. Possible decays such as  $Z \rightarrow \chi\bar{\chi}$  or  $H \rightarrow 2\chi 2\bar{\chi}$  could lead to the production of an FCP in this parameter space.

This pocket was not explored in the CMS 13 TeV search due to a transverse momentum threshold of  $p_T > 50 \text{ GeV}$ . Targeted searches at CMS lowering the  $p_T$  threshold could probe this currently unconstrained space.

### 3. Improving reliability of cosmological bounds

While the more reliable DD searches have taken precedent in this project, Fig. 1 clearly shows that cosmological bounds exclude **all**  $q/e < 1$  for  $m < 550$  GeV. The verification of the assumptions underlying the XENON-nT search would achieve the same end as suggestions 1 and 2. In practice, this would require probing both the age of the universe (pre-BBN) and temperatures up to the relevant FCP masses. This would be extremely difficult compared to improving collider bounds.

### 4. Higher-energy future colliders

Should the regions discussed above be excluded with greater confidence, the natural next step is to extend searches to higher energies. If future experiments exclude FCPs with  $q = \frac{1}{6}e$  up to the current mass limits for  $q = \frac{1}{3}e$ , then an FCP discovery in this regime would constitute the heaviest elementary particle observed to date.

However, the LHC is nearing its energy limit, now focusing primarily on increased luminosity rather than centre-of-mass energy. To probe higher masses, next-generation colliders will be essential. The proposed FCC at CERN, for example, would dramatically extend the FCP masses that can be probed. Unfortunately, the timescale is discouraging - a decision will be made on the FCC in 2028, and it would only become fully operational in 2070 [20].

## References

- [1] R. A. Millikan “On the Elementary Electrical Charge and the Avogadro Constant”, *Phys. Rev.* **109** (1913).
- [2] Wikipedia - Group (mathematics).
- [3] V. Bouchard, MA PH 464 - Group Theory in Physics: Lecture Notes.
- [4] R. Alonso *et al.* , “Fractional-charge hadrons and leptons to tell the Standard Model group apart”, 2024.
- [5] S. Cléry *et al.* , “Did the Laws of Physics Emerge at  $t = 10^{34}$ s? Inflation, Reheating and Particle Creation in the Very Early Universe”, 2025.
- [6] The CMS Collaboration, “Search for fractionally charged particles in proton-proton collisions at  $\sqrt{s} = 13$  TeV”, *Phys. Rev. Lett.* **134** (2025).
- [7] The CMS Collaboration, “Search for fractionally charged particles in pp collisions at  $\sqrt{s} = 7$  TeV”, *Phys. Rev. D* **86** (2013)
- [8] The CMS Collaboration, “Erratum: Search for fractionally charged particles in  $pp$  collisions at  $\sqrt{s}=7$  TeV”, *Phys. Rev. D* **106** (2022)
- [9] A.A. Prinz *et al.* , “Search for Millicharged Particles at SLAC”, *Phys. Rev. Lett.* **81** (1998).

- [10] A. Ball *et al.* , “Search for millicharged particles in proton-proton collisions at  $\sqrt{s} = 13$  TeV”, *Phys. Rev. D* **102** (2020).
- [11] S. Alcott *et al.* , “Search for millicharged particles in proton-proton collisions at  $\sqrt{s} = 13.6$  TeV”, *Phys. Rev. D* **102** (2020).
- [12] R. Acciarri *et al.* , “Improved Limits on Millicharged Particles Using the ArgoNeuT Experiment at Fermilab”, *Phys. Rev. Lett* **124** (2020).
- [13] SENSEI Collaboration, “Search by the SENSEI Experiment for Millicharged Particles Produced in the NuMI Beam ”, *Phys. Rev. Lett* **133** (2024) 071801.
- [14] G. Magill, R. Plestid, M. Pospelov and Y. Tsai , “Millicharged Particles in Neutrino Experiments”, *Phys. Rev. Lett* **122** (2019) 071801.
- [15] G. Marocco, S. Sarkar, “Blast from the past: Constraints on the dark sector from the BEBC WA66 beam dump experiment” , *SciPost Phys.* **10** (2021) 043.
- [16] TEXONO Collaboration, “Constraints on millicharged particles with low-threshold germanium detectors at Kuo-Sheng Reactor Neutrino Laboratory”, *Phys. Rev. D* **99** (2019) 032009.
- [17] Z. Zhang, J. Hu, X. Geng and F. Liu, “Search for fractionally charged particles as lightly ionizing particles using public data from an underground direct detection experiment ”, arXiv:2502.02894.
- [18] S. Davidson, S Hannestad and G. Raffelt, “Updated bounds on milli-charged particles”, *JHEP* **05** (2000) 003.
- [19] D. Forbes, Y. Kahn and R. Nguyen, “Exotic particles at the DUNE near detector from charged pion scattering”, *Phys. Rev. D* **110** (2024) 095029.
- [20] The Future Circular Collider, CERN.

## 6 Appendix

Calculations were made by prioritising intuitive, easier to understand techniques over rigorous mathematical methods were necessary.

The generators for both SU(2) and SO(3) were calculated as follows. First, we impose the unitary condition on the group element in exponential form:

$$U^\dagger U = \mathbb{I} \implies (e^{i\alpha T})^\dagger (e^{i\alpha T}) = \mathbb{I} \implies (i\alpha T)^\dagger = -i\alpha T$$

This last step should be approached with caution - it does not always necessarily hold, but it is fine here because  $T^\dagger$  and  $T$  are similar, and we are working in the setting of Lie groups. Thus we obtain our condition

$$(iT)^\dagger = -(iT) \implies T^\dagger = T$$

i.e.  $T$  is hermitian. We can then write  $T$  as  $\begin{bmatrix} a & b \\ \bar{b} & c \end{bmatrix}$ , with  $a, c \in \mathbb{R}$ . Next, we can impose the condition that  $\det(T) = 1$ , by Taylor expanding to the first order.

$$\det(e^{i\alpha T}) = 1 \implies \det(\mathbb{I} + i\alpha T) = 1 \implies \det \begin{pmatrix} 1+a & b \\ \bar{b} & 1+c \end{pmatrix} = 1$$

And hence, we can expand and approximate to the first order

$$(1+a)(1+c) - b\bar{b} = 1 \approx 1 + a + c \implies a = -c$$

So we know our generators are of form  $T = \begin{bmatrix} a & b \\ \bar{b} & -a \end{bmatrix}$ . It is not hard, then, to find a basis that fits these conditions. In fact, this basis is the set of pauli matrices

$$\left\{ \begin{bmatrix} 0 & 1 \\ 1 & 0 \end{bmatrix}, \begin{bmatrix} 0 & -i \\ i & 0 \end{bmatrix}, \begin{bmatrix} 1 & 0 \\ 0 & -1 \end{bmatrix}, \right\}$$

which are denoted  $\sigma_i, i \in \{1, 2, 3\}$ .